Journal of Radiation Research, Vol. 67, No. 5, 2026, pp. 770–778
https://doi.org/10.1093/jrr/rrag075
Advance Access Publication: 21 September 2026

Effects of X-ray and carbon-ion beam irradiation on pathological cardiac remodeling in mice

Naoko Okano[1,2,*,‡], Nozomi Furukawa[3,‡], Norimichi Koitabashi[3], Hiromu Suda[1], Yukari Yoshida[1], Hideki Ishii[3] and Tatsuya Ohno[1]

[1]Gunma University Heavy Ion Medical Center (GHMC), 3-39-15 Showa-machi Maebashi, Gunma 371-8511, Japan
[2]Juntendo University Nerima Hospital, Radiology department, 3-1-10 Takano-dai, Nerima, Tokyo 177-8521, Japan,
[3]Department of Cardiovascular Medicine, Gunma University Graduate School of Medicine, 3-39-15 Showa-machi Maebashi, Gunma 371-8511, Japan
[*]Corresponding author. Gunma University Heavy Ion Medical Center (GHMC), 3-39-15 Showa-machi Maebashi, Gunma 371-8511, Japan.
Fax: +81-27-220-8345; Email: okano.n@gunma-u.ac.jp; n.okano.cm@juntendo.ac.jp
[‡]Naoko Okano and Nozomi Furukawa contributed equally.
(Received 13 October 2025; revised 4 February 2026; accepted 21 July 2026)

ABSTRACT

The objective of this study was to evaluate the effects of X-ray and carbon-ion (C-ion) beam irradiation on murine hearts under both normal and pathological conditions. Pathological cardiac hypertrophy was induced in mice by transverse aortic constriction (TAC) surgery. The control and TAC groups were irradiated with 30 Gy of X-rays or C-ion beams. Cardiac function was assessed every two weeks using echocardiography. Fibrosis, cardiomyocyte hypertrophy and *Nppb* expression were evaluated 8 weeks post-TAC. Irradiation had a limited effect on heart weight and function in control mice, although Nppb levels were elevated. TAC mice exhibited functional decline and increased fibrosis, which were improved by C-ions but not X-rays. Irradiation improved cardiac function and fibrosis in mice with heart failure, suggesting potential cardioprotective benefits. At the same physical dose, C-ion irradiation showed a trend toward improved cardiac function and reduced fibrosis; however, these differences were not significant compared with X-rays.

Keywords: heart failure; carbon-ion; X-ray; cardiac function; mice

INTRODUCTION

Heart failure (HF) is a clinical syndrome characterized by dyspnea, fatigue, edema and exercise intolerance owing to cardiac dysfunction and inadequate compensatory mechanisms that maintain cardiac pump function. The global prevalence of HF continues to rise, and despite advances in therapeutic approaches, it remains a life-threatening condition [1–5]. Therefore, innovative treatment strategies are urgently required.

Radiation therapy has long been recognized as a cause of cardiac injury, and the heart has traditionally been regarded as a critical organ at risk during thoracic irradiation [6–13]. In a landmark case–control study, Darby *et al.* established a linear dose–response relationship with no apparent threshold, showing that major coronary events increased by 7.4% per Gy (95% confidence interval [CI]: 2.9–14.5%), and this increase began within 5 years of radiotherapy and continued for at least 20 years [6]. In addition to the aforementioned report, large-scale epidemiological studies and experimental investigations have demonstrated that conventional X-ray radiotherapy can induce ischemic heart disease, myocardial fibrosis and long-term cardiac dysfunction in a dose-dependent manner [6–15]. These findings indicate that radiation-induced heart disease is an important and clinically relevant disease.

In contrast to these detrimental effects, recent technological advances have enabled highly precise and focal irradiation of cardiac tissue, leading to the emergence of cardiac radioablation as a novel therapeutic approach. Clinical studies have demonstrated that targeted X-ray irradiation can effectively suppress refractory ventricular and atrial arrhythmias, with acceptable short-term safety profiles [16–18]. Moreover, accumulating experimental and clinical evidence suggests that cardiac irradiation may exert beneficial effects on cardiac function and remodeling in selected pathological settings, including cardiomyopathy and HF [19–21]. These observations

© The Author(s) 2026. Published by Oxford University Press on behalf of The Japanese Radiation Research Society and Japanese Society for Radiation Oncology.
This is an Open Access article distributed under the terms of the Creative Commons Attribution-NonCommercial License (https://creativecommons.org/licenses/by-nc/4.0/), which permits non-commercial re-use, distribution, and reproduction in any medium, provided the original work is properly cited. For commercial re-use, please contact reprints@oup.com for reprints and translation rights for reprints. All other permissions can be obtained through our RightsLink service via the Permissions link on the article page on our site—for further information please contact journals.permissions@oup.com.

highlight the context-dependent nature of radiation effects on the heart.

Compared with conventional X-rays, particle beams such as carbon-ions (C-ion) offer a more precise dose distribution and better sparing of surrounding normal tissues. These properties may reduce the incidence of adverse events, especially in patients with multiple comorbidities, representing a major clinical advantage [22–26]. In the cardiovascular field, preclinical studies have shown that C-ion irradiation favorably modulates electrical remodeling, gap junction expression and autonomic innervation, thereby reducing vulnerability to atrial and ventricular arrhythmias [27–32]. In addition, clinical case reports have described antiarrhythmic effects in refractory arrhythmias after incidental cardiac exposure to C-ion beams during radiotherapy for mediastinal tumors, as well as after C-ion irradiation delivered in a stereotactic body radiation therapy-like manner for treating arrhythmias [33, 34].

At the molecular level, several mechanisms have been implicated in the development and progression of HF, including DNA single-strand breaks, impaired DNA damage repair pathways, and the release of damage-associated molecular patterns such as high-mobility group box 1 (HMGB1) [35, 36]. Radiation-induced DNA damage and HMGB1 release are well-established phenomena in tumor biology and immuno-radiobiology [37], and these pathways may also contribute to radiation-induced cardiac remodeling. Importantly, whether such molecular responses lead to detrimental injury or adaptive remodeling may depend on radiation quality, dose distribution and underlying pathological state of the myocardium.

Despite the growing interest in cardiac radioablation and particle beam therapy, the effects of radiation quality on pathological cardiac remodeling under pressure overload remain poorly understood. In particular, direct experimental comparisons between conventional X-ray and C-ion irradiation in normal and failing hearts are limited. Therefore, we aimed to investigate the effects of X-ray and C-ion beam irradiation on cardiac structure and function in a murine model under physiological conditions and pressure overload–induced pathological remodeling.

MATERIALS AND METHODS

Animals

All animal experiments were performed in accordance with protocols approved by the Animal Care and Experimentation Committee of Gunma University (19–076). Male C57BL/6JJcl mice were purchased from CLEA Japan Inc. (Tokyo, Japan) and housed in a temperature-controlled environment with a 12-hour light/dark cycle. Standard laboratory chow (CE-2; CLEA Japan) and water were provided *ad libitum*.

Pressure overload–induced cardiac remodeling

Pathological cardiac remodeling was induced by transverse aortic constriction (TAC) surgery [38], a well-established murine model of pressure overload. Briefly, the thoracic aorta was accessed via a minimal sternal incision, and a 7–0 suture was tied around the vessel using a 26-gauge needle to ensure consistent constriction. To minimize variability related to body size and developmental stage, TAC surgery was performed only in mice aged 8–12 weeks and weighing 23–26 g at the time of surgery; mice that did not meet these criteria were excluded from the TAC procedure and subsequent analyses. The control mice were age-matched with the TAC group. TAC initially induces adaptive concentric hypertrophy, which subsequently progresses to left ventricular (LV) dilation and systolic dysfunction over a period of 2–4 weeks, thereby modeling pressure overload–induced HF [39, 40].

Echocardiography was performed every 2 weeks following TAC to monitor cardiac structure and function. Irradiation was performed 2 weeks after TAC, when pathological remodeling had developed but before end-stage HF [39]. Echocardiographic assessments were conducted without anesthesia to avoid depressant effects on cardiac function [41].

Irradiation protocols

Irradiation was performed at the 2-week post-TAC time point, when HF typically develops. Following induction of intraperitoneal anesthesia with ketamine and xylazine, each mouse was secured in the supine position on an acrylic plate to align the heart with the irradiation field.

X-ray irradiation was performed using a high-power X-ray generator (TITAN-225 s, Shimadzu Industrial Equipment Systems, Shiga, Japan), operated at 200 kVp, 14.6 mA, a 0.5 mm aluminum +0.5 mm copper filter, and a dose rate of 1.08 Gy/min. Mice were irradiated with 30 Gy delivered in a single fraction, from 0°, with a 10-mm slit lead plate shielding all tissues outside the cardiac field.

C-ion irradiation was performed at Gunma University Heavy Ion Medical Center, using a beam energy of 290 MeV/nucleon, a 6-cm spread-out Bragg peak (SOBP), and an average linear energy transfer at the center of a 6-cm SOBP of approximately 50 keV/μm. The irradiation field (1 × 12 cm) was shaped using a collimator. The beam range was adjusted using a variable-water-thickness phantom to remove the proximal 5 cm of the 6-cm SOBP beam. C-ion irradiation was delivered from 0° in the anterior–posterior direction. Simulation analyses confirmed that this irradiation method provided sufficient cardiac coverage in terms of dose distribution across the full cardiac depth range (Supplementary Fig. 1). Positioning was performed by aligning the laser with the center of the irradiation field along the midline of the heart. Subsequently, fluoroscopic imaging was performed to confirm that the heart was within the irradiation field prior to irradiation (Supplementary Fig. 2).

Irradiation dose

For X-ray radioablation of refractory arrhythmias, a single fraction of 25 Gy has been used [16, 17]. Accordingly, preliminary experiments were conducted using four irradiation patterns: X-rays at 20 and 30 Gy; C-ion beams at 30 Gy (physically equivalent to X-rays); and C-ion beams at 10 Gy (relative biological effectiveness [RBE]-adjusted dose equivalent to X-rays) [42]. These preliminary experiments evaluated outcomes at 2 weeks post-irradiation.

Echocardiographic evaluation and tissue sampling

Transthoracic echocardiography (EUB-7500; Hitachi Medical Systems, Tokyo, Japan) was performed on conscious mice at 2 weeks post-TAC and subsequently every 2 weeks after irradiation for up to 8 weeks. M-mode images were used to measure the left ventricular end-diastolic (LVDd) and end-systolic (LVDs) dimensions averaged over three to five cardiac cycles. FS and LVM were calculated as previously described [41]. All studies and analyses were performed in a blinded manner with respect to the experimental group assignment. Eight

weeks post-irradiation, the mice were euthanized under isoflurane anesthesia. Blood samples were collected, and body weight (BW), heart weight (HW) and tibial length were recorded. The hearts were snap-frozen in liquid nitrogen for RNA analysis or fixed in 10% formalin for histological examination.

Histological analysis

The following analyses were performed using cardiac tissues collected 8 weeks post-irradiation. Immunofluorescence staining and analysis were performed as previously described [41, 43]. Briefly, hearts were embedded in paraffin and sectioned at a thickness of 2 μm. Masson's trichrome staining was used to assess myocardial fibrosis. Six nonoverlapping fields from the mid-LV short axis were imaged at 20× magnification. The fibrotic area (%) was quantified using the WinROOF 2018 software (Mitani Corporation, Tokyo, Japan).

To analyze cardiomyocyte hypertrophy, sections were co-stained with Alexa Fluor 488-conjugated wheat germ agglutinin (WGA) and Alexa Fluor 568-conjugated isolectin B4 (GS-IB4). After antigen retrieval (Dako), sections were incubated overnight at 4°C. Cardiomyocyte cross-sectional area (CSA) and capillary density were quantified using WGA-stained myocardial sections. Measurements were performed in identical microscopic fields using fluorescence microscopy and semi-automated image analysis software (WinROOF, 2018). Cardiomyocytes with clearly delineated cell borders and identifiable capillaries were selected for analysis. Approximately 400–800 cardiomyocytes per sample were analyzed. Representative images illustrating the measurement strategy are shown in Supplementary Fig. 4.

RNA isolation and reverse transcription–quantitative PCR

The following analyses were performed using cardiac tissue collected 8 weeks post-irradiation. Total RNA was extracted from the cardiac tissue using ISOGEN reagent (Takara Bio, Kyoto, Japan), and 1 μg of RNA was reverse-transcribed using the RNA LA PCR Kit (Takara Bio), followed by quantitative real-time PCR using THUNDERBIRD SYBR qPCR Mix (TOYOBO, Osaka, Japan) and an MX3000P system (Stratagene, USA). *Nppb* mRNA expression was normalized to that of GAPDH.

Statistical analysis

Group comparisons were conducted using repeated-measures analysis of variance (ANOVA) or an unpaired, two-tailed Student's *t*-test. ANOVA was performed using R version 4.4.2 (R Foundation for Statistical Computing, Vienna, Austria), and *t*-tests were performed using SPSS version 26.0 (IBM Corp., Armonk, NY, USA) [44]. Statistical significance was set at $P < 0.05$.

RESULTS

Group assignment

Mice were assigned to one of six groups ($n = 5$/group): non-irradiated (Cont), X-ray-irradiated (Cont+X), and carbon-ion-irradiated (Cont+C) for the control cohort, and non-irradiated (TAC), X-ray-irradiated (TAC + X), and carbon-ion-irradiated (TAC + C) for the TAC cohort. Before the TAC procedure, there were no significant differences in BW or cardiac function among the groups ($P > 0.05$), except for the LVDd. Notably, LVDd differed significantly only between the TAC + X and Cont groups, and between the TAC + C and Cont groups before treatment ($P < 0.01$).

Determination of irradiation dose

Regarding cardiac function, the C-ion irradiation group showed a trend toward improved FS at 2 weeks post-irradiation, with a more pronounced improvement at 30 Gy than at 10 Gy. In the X-ray irradiation group, no significant difference was observed between 20 and 30 Gy. Although improvement was observed at 1 week post-irradiation, cardiac function slightly worsened at 2 weeks (Supplementary Fig. 3A). Additionally, LVM showed a trend toward improvement in the C-ion group but not in the X-ray group (Supplementary Fig. 3B). Because establishing equivalent doses while accounting for the RBE was challenging, a physical dose of 30 Gy was selected for both X-rays and C-ions in this study.

Cardiac function

The trends in echocardiographic parameters are shown in Fig. 1. Comparisons between the Cont and TAC groups under non-irradiated conditions are presented. At the pre-irradiation time point (2 weeks post-TAC), unpaired *t*-tests showed that FS, LVDs and LVM significantly worsened in the TAC group relative to the Cont group, whereas LVDd did not differ significantly (Fig. 1). Comparing the trend using repeated-measures ANOVA, FS, LVDd and LVDs were significantly or slightly worsened in the TAC group compared with the Cont group, whereas no significant change was observed in LVM (Fig. 1). Although universally accepted normal ranges have not been established for murine echocardiographic parameters, the observed echocardiographic profile was consistent with pressure overload–induced pathological remodeling at a compensated-to-early-decompensated stage, rather than overt end-stage HF.

Results comparing the effects of irradiation within the control groups are shown in Fig. 1. At the pre-irradiation time point, no statistically significant differences were detected across any parameters among the Cont, Cont+X and Cont+C groups. In the repeated-measures trend analysis, only LVM worsened in the Cont+X group compared with the Cont group, with no significant differences observed between the Cont+X and Cont+C groups (Fig. 1).

Additionally, results comparing the effects of irradiation within TAC groups are presented in Fig. 1. At the pre-irradiation time point, no statistically significant differences were detected across any parameters among the TAC and TAC + C groups. The TAC + X group showed significantly lower LVDd and LVM than the TAC group, whereas no significant differences were observed in FS and LVDs (Fig. 1). In the repeated-measures trend analysis, only FS was improved in the TAC + C group compared with the TAC or TAC + X groups, and no significant between-group differences were observed for the other echocardiographic parameters (Fig. 1).

Heart weight

The HW–to–BW ratio (HW/BW) at 8 weeks post-irradiation is shown in Fig. 2. Under the non-irradiated condition, HW/BW was significantly higher in the TAC group than in the Cont group. Within

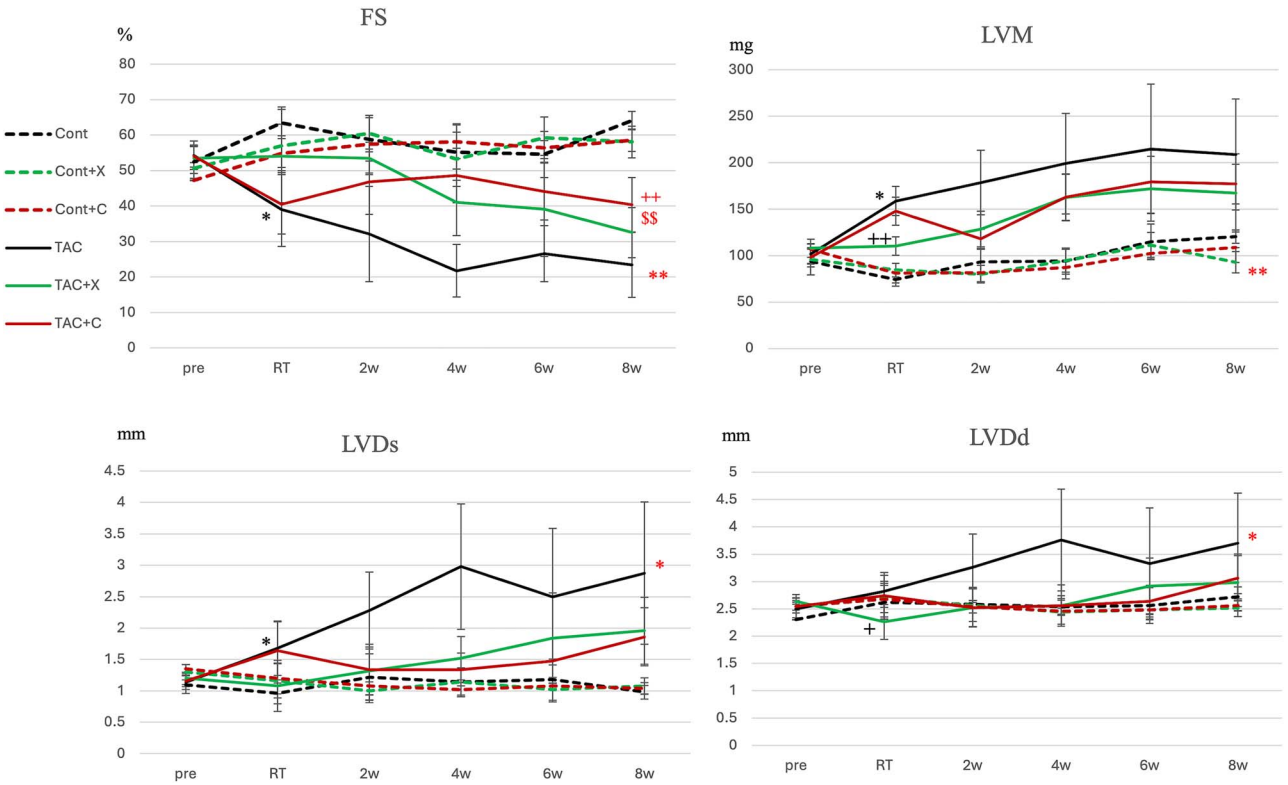


Fig. 1. Echocardiographic trends: Pre-treatment, pre-irradiation, and every 2 weeks up to 8 weeks post-irradiation. Mice were age- and weight-matched at the time of TAC surgery. Heart condition: Normal line, TAC group; broken line, control group. Irradiation conditions: Black, non-irradiation; green, X-ray irradiation; red, C-ion irradiation. (A) LV percent fractional shortening (FS). (B) LV mass (LVM). (C) Left ventricular end-systolic dimension (LVDs). (D) Left ventricular end-diastolic dimension (LVDd). (Supplementary Fig. 5 shows ratio to pre-treatment level). At pre-irradiation time point comparisons were performed using unpaired, two-tailed Student's *t*-test written in black. Group comparisons were performed using repeated measurements ANOVA written in red. $^{*}P < 0.05$ vs Control without irradiation; $^{**}P < 0.01$ vs Control without irradiation; $^{+}P < 0.05$ vs TAC without irradiation; $^{++}P < 0.01$ vs TAC without irradiation; $^{\$\$}P < 0.01$ vs TAC with X-ray irradiation.

the control groups, although no significant difference was observed between Cont+X and Cont, HW/BW was significantly higher in the Cont+C than in the Cont group. No significant differences were observed between the Cont+X and Cont+C groups or among the TAC groups (Fig. 2). However, HW/BW was significantly higher in the TAC, TAC + X, and TAC + C groups than in the Cont group (Fig. 2).

Fibrosis and cardiomyocyte hypertrophy

Myocardial fibrosis at 8 weeks post-irradiation is shown in Fig. 3A and B. Under the non-irradiated condition, myocardial fibrosis was significantly increased in the TAC group compared with the Cont group. Within the control groups, no significant differences were observed among the Cont+X, Cont+C and Cont groups (Fig. 3B). In addition, no significant differences were observed among the TAC groups (Fig. 3B). However, myocardial fibrosis was significantly increased in the TAC and TAC + X groups compared with the Cont group, whereas no significant difference was observed between the TAC + C and Cont groups (Fig. 3B).

Cardiomyocyte size at 8 weeks post-irradiation is shown in Fig. 3A and 3C. Under the non-irradiated condition, cardiomyocyte size was significantly increased in the TAC group compared with the Cont group, indicating TAC-induced cardiomyocyte hypertrophy (Fig. 3C). Within the control groups, no significant differences were observed among the Cont+X, Cont+C and Cont groups (Fig. 3C). In addition, no significant differences were observed between TAC + X and TAC and between TAC + X and TAC + C (Fig. 3C). However, cardiomyocyte size was modestly reduced in the TAC + C group compared with the TAC group (Fig. 3C).

RNA expression analysis

Expression of *Nppb*, a marker of cardiac stress, at 8 weeks post-irradiation is shown in Fig. 4. Under the non-irradiated condition, *Nppb* expression was significantly higher in the TAC group than in the Cont group. Within the control groups, Nppb expression was significantly elevated in the Cont+X and Cont+C groups compared with the Cont group ($P < 0.01$ and $P = 0.043$, respectively) (Fig. 4). In addition, Nppb expression was significantly higher in the Cont+X

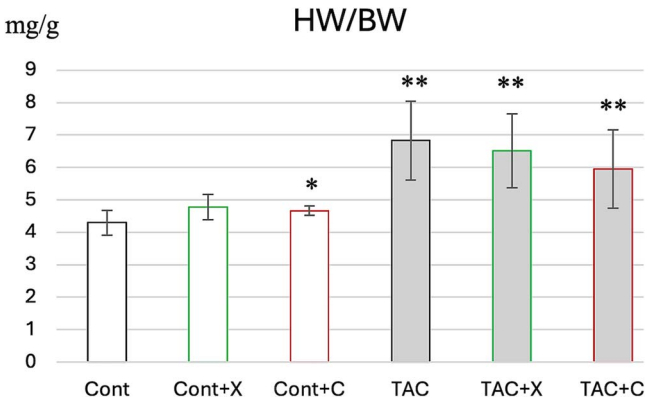


Fig. 2. Average HW ($n = 5$ mice/group) at 8 weeks post-irradiation. HW/BW ratio. $^{*}P < 0.05$; $^{**}P < 0.01$ vs control without irradiation.

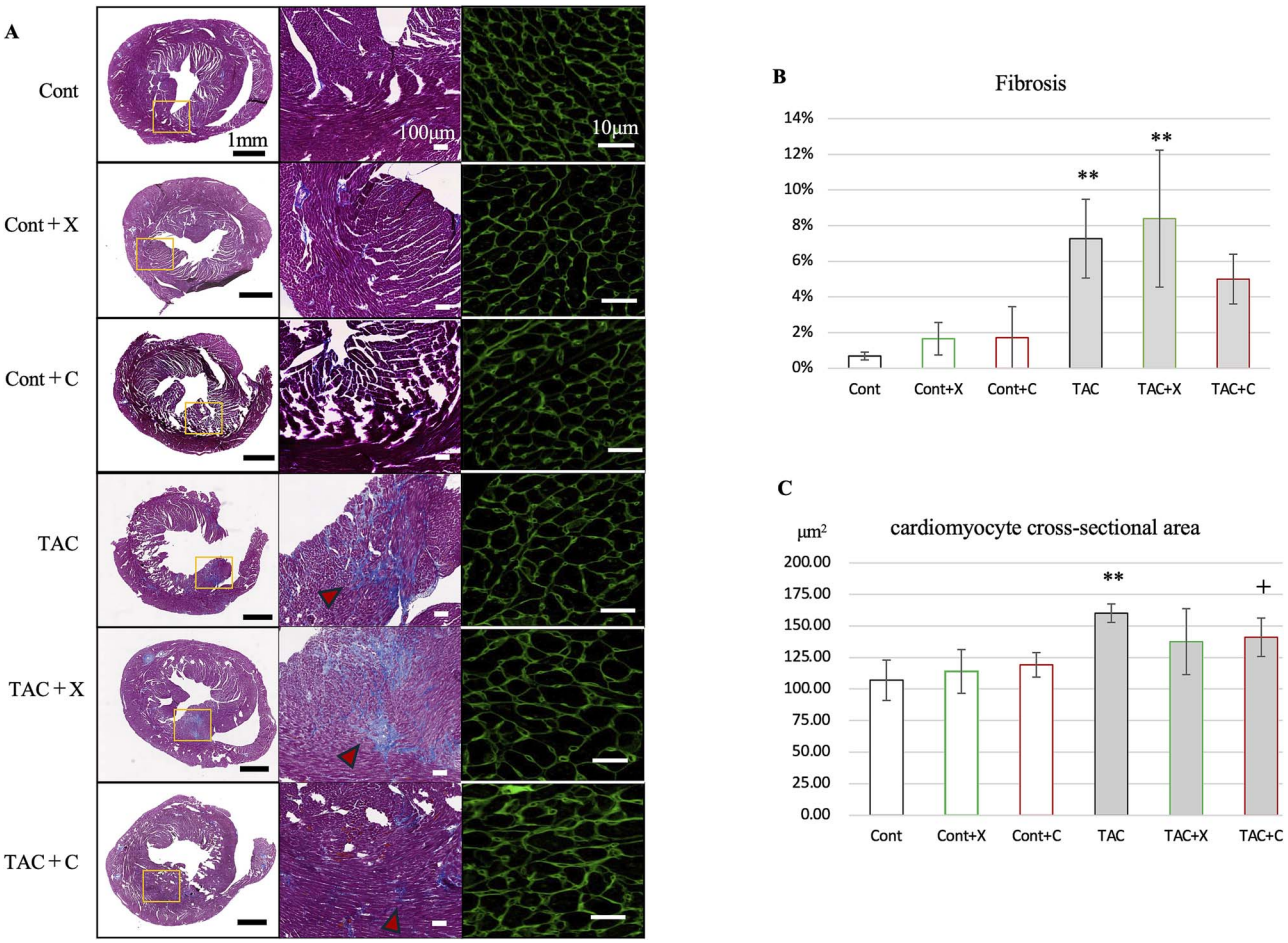


Fig. 3. Histological findings at 8 weeks post-irradiation. (A) Left, middle: Representative microscopic image of cardiomyocytes in a tissue cross-section stained with Masson trichrome. Cardiomyocytes stained red, fibrotic area stained blue and pointed by red arrow. Scale bars: 1 mm and 100 μm. Right: Representative microscopic image of cardiomyocytes in a tissue cross-section stained with WGA. The identification of cardiomyocytes is shown in Supplementary Fig. 4. Scale bars: 10 μm. (B) Mean CSA obtained by Masson trichrome staining. (C) Median CSA obtained by WGA staining. $^{*}P < 0.05$, $^{**}P < 0.01$ vs control without irradiation, $^{+}P < 0.05$ vs TAC without irradiation.

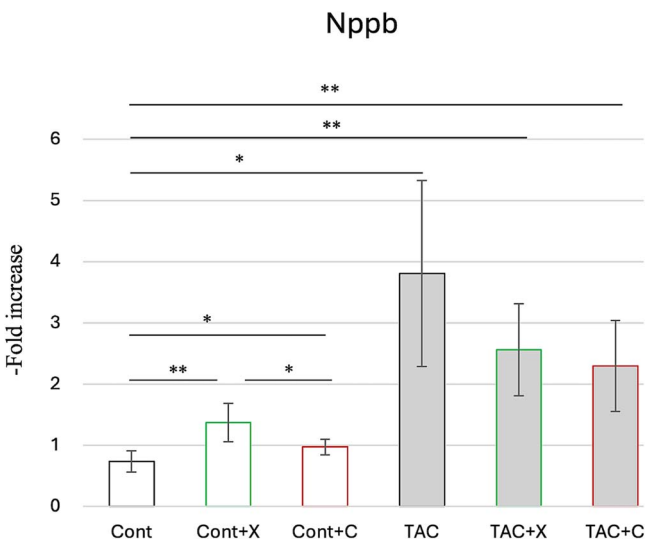


Fig. 4. mRNA levels were assessed by reverse transcription–quantitative PCR (RT-qPCR) and normalized to *Gapdh* and then to the control group without irradiation. $^{*}P < 0.05$; $^{**}P < 0.01$. Exact *P*-values are provided in the results section for each comparison.

group than in the Cont+C group ($P = 0.043$) (Fig. 4). Among the TAC groups (TAC, TAC + X, and TAC + C), no significant differences were observed between any pairwise comparisons. However, Nppb expression was significantly higher in all TAC groups compared with the Cont group (all $P < 0.01$) (Fig. 4).

DISCUSSION

In the current study, we investigated the effects of focal cardiac irradiation with X-rays and C-ion beams in mice under physiological conditions and pressure overload–induced pathological remodeling. The principal findings were as follows: (i) in normal hearts, neither irradiation modality caused overt deterioration of cardiac function during the observation period; (ii) TAC-induced pressure overload resulted in impaired cardiac function and increased myocardial fibrosis; and (iii) under these pathological conditions, C-ion irradiation, but not X-ray irradiation, was associated with an improvement in systolic function and attenuation of fibrotic remodeling. These findings indicate that cardiac responses to irradiation are highly context-dependent and may differ qualitatively according to the radiation modality.

In normal hearts, exposure to X-rays was associated with a substantial reduction in LVM at the end of the observation period; however, no irradiation-induced changes in cardiac function, heart size, fibrosis or cardiomyocyte hypertrophy were observed following X-ray or C-ion exposure. *Nppb* expression was increased in both the X-ray and C-ion irradiation groups compared with the non-irradiated group, with a substantially greater increase in the X-ray group. Saiki et al. reported cardiac function and histological findings at 30 weeks after internal irradiation with I-131 in mice [15]. The authors found that, although systolic function, including ejection fraction (EF), was preserved, diastolic dysfunction was observed along with myocardial fibrosis, cardiomyocyte hypertrophy and decreased microvascular density, suggesting the potential development of HF without reduced EF. In the current study, no significant differences were observed, except for impaired relaxation; however, the overall trends were similar. The lack of significant differences may be attributable to the small sample size and relatively short observation period. Additionally, a trend toward decreased *Nppb* expression was observed after C-ion irradiation; however, this finding cannot be fully explained based on the current results alone, and long-term follow-up is warranted.

Pedersen et al. reported that 5 Gy irradiation improved multiple HF parameters in mouse models induced by metabolic stress, ischemia or pressure overload. Disease progression was assessed at 3, 6, 12 and 15 weeks post-irradiation [19]. Although the irradiation dose and follow-up period differed from those in the present study, the improvement in cardiac function (e.g. FS) observed in the TAC group was consistent with findings reported in other studies. Accordingly, irradiation may exert beneficial effects in diseased hearts. However, comparable data for C-ions are lacking, and long-term outcomes and dose-dependent effects require further investigation.

Regarding myocardial fibrosis, TAC-induced pressure overload resulted in a marked increase in fibrotic remodeling, consistent with previous reports. Although X-ray irradiation did not mitigate this response, fibrosis was attenuated in the C-ion–irradiated TAC group. Previous studies have reported variable effects of cardiac irradiation on fibrosis, with some showing improvement post-irradiation and others demonstrating minimal or dose-independent changes [19, 31, 45]. The present findings extend these observations by suggesting that the fibrotic response may be modulated by radiation modality, although the underlying mechanisms remain to be elucidated.

Regarding cardiomyocyte hypertrophy, cellular enlargement was evident in TAC-induced hearts, whereas hypertrophy was less pronounced in the irradiated groups. Myocardial fibrosis and cardiomyocyte hypertrophy were evaluated using cross-sectional histological images obtained at identical mid-LV levels. Nuclear staining and corrected scale calibration were applied to ensure accurate assessment

of the cardiomyocyte CSA and myocardial architecture. Although the differences in cardiomyocyte size did not reach statistical significance across all comparisons, the trend toward reduced hypertrophy in the C-ion–irradiated hearts paralleled the observed functional improvement. Previous studies have suggested that irradiation modulates pathways involved in fibrotic and hypertrophic remodeling [19], and similar mechanisms may underlie the effects observed in the present study.

At the molecular level, radiation induces DNA damage responses and triggers the release of damage-associated molecular patterns, such as HMGB1, which have also been implicated in the development and progression of HF [35–37]. Importantly, activation of these pathways may not necessarily be detrimental. Depending on the pathological context, timing and radiation quality, such responses may contribute to adaptive remodeling or modulation of inflammatory and fibrotic signaling. In the present study, although *Nppb* expression did not differ significantly among the TAC groups, the overall functional and histological profile suggests that C-ion irradiation may induce qualitatively distinct myocardial responses compared with X-ray irradiation.

In this study, a direct biological comparison between X-rays and C-ions was not performed. Although we selected physically equivalent doses, this does not imply biological equivalence. Differences in factors such as biological effectiveness and dose distribution may have influenced the observed results [42]. Therefore, comparisons under biologically equivalent conditions should be addressed in future studies. Accordingly, direct biological equivalence between the two modalities cannot be assumed. Instead, our findings indicate that radiation quality influences cardiac remodeling under pressure overload conditions, with C-ion irradiation associated with improved systolic function and attenuation of myocardial fibrosis compared with X-ray irradiation.

Limitations

This study has several limitations. First, the degree of functional impairment in the TAC + X-ray group was relatively mild, which may have limited our ability to detect potential beneficial effects of X-ray irradiation. Second, direct comparisons between radiation modalities are limited by the lack of established cardiac-specific RBE values, particularly under pathological conditions. Third, escalation of the X-ray dose beyond 30 Gy was not feasible owing to practical constraints related to anesthesia and procedural duration. Fourth, cardiomyocyte CSA was assessed by WGA staining without nuclear counterstaining. Although consistent staining and analysis criteria were applied across all groups, this approach may have limited the precise identification of individual cardiomyocytes. Finally, the sample size was relatively small, and the study may have been underpowered to detect modest differences in molecular endpoints such as *Nppb* expression.

CONCLUSION

In conclusion, focal cardiac irradiation exerted minimal effects on normal hearts but produced distinct responses in pressure overload–induced pathological remodeling. C-ion irradiation, but not X-ray irradiation, was associated with improved systolic function and attenuation of myocardial fibrosis in failing hearts. These findings suggest that the radiation quality may critically influence cardiac remodeling under pathological stress and highlight the potential of C-ion beam therapy as a novel modality for modulating cardiac dysfunction in selected disease contexts.

ACKNOWLEDGEMENTS

We thank Tomoko Yako (GHMC) and Miki Matsui (Department of Cardiovascular Medicine, Gunma University) for technical assistance. We also thank Bioedit Ltd and Editage for English editing.

SUPPLEMENTARY DATA

Supplementary data is available at *Journal of Radiation Research* online.

CONFLICT OF INTEREST

N.O. and T.O. received an honorarium from Hitachi Industries. The other authors have no conflicts of interest directly relevant to the content of this article.

FUNDING

This work was supported by a Grant-in-Aid for Scientific Research, for Young Scientists (20 K16719).

PRESENTATION AT A CONFERENCE

This research was presented at the 37th Annual Meeting of the Japanese Society for Radiation Oncology.

REFERENCES

1. Ambrosy AP, Fonarow GC, Butler J *et al.* The global health and economic burden of hospitalizations for heart failure: lessons learned from hospitalized heart failure registries. *J Am Coll Cardiol* 2014;63:1123–33. https://doi.org/10.1016/j.jacc.2013.11.053.
2. Lloyd-Jones DM, Larson MG, Leip EP *et al.* Lifetime risk for developing congestive heart failure: the Framingham heart study. *Circulation* 2002;106:3068–72. https://doi.org/10.1161/01.CIR.0000039105.49749.6F.
3. Go AS, Mozaffarian D, Roger VL *et al.* Heart disease and stroke statistics—2014 update: a report from the American Heart Association. *Circulation* 2014;129:e28–292. https://doi.org/10.1161/01.cir.0000441139.02102.80.
4. Shimokawa H, Miura M, Nochioka K *et al.* Heart failure as a general pandemic in Asia. *Eur J Heart Fail* 2015;17:884–92. https://doi.org/10.1002/ejhf.319.
5. Heidenreich PA, Bozkurt B, Aguilar D *et al.* 2022 AHA/ACC/HFSA guideline for the management of heart Failure: executive summary: a report of the American College of Cardiology/American Heart Association Joint Committee on Clinical Practice Guidelines. *Circulation* 2022;145:e876–94. https://doi.org/10.1161/CIR.0000000000001062.
6. Darby SC, Ewertz M, McGale P *et al.* Risk of ischemic heart disease in women after radiotherapy for breast cancer. *N Engl J Med* 2013;368:987–98. https://doi.org/10.1056/NEJMoa1209825.
7. Aleman BMP, van den Belt-Dusebout AW, Klokman WJ *et al.* Long-term cause-specific mortality of patients treated for

Hodgkin's disease. *J Clin Oncol* 2003;21:3431–9. https://doi.org/10.1200/JCO.2003.07.131.
8. Bouillon K, Haddy N, Delaloge S *et al.* Long-term cardiovascular mortality after radiotherapy for breast cancer. *J Am Coll Cardiol* 2011;57:445–52. https://doi.org/10.1016/j.jacc.2010.08.638.
9. van Nimwegen FA, Schaapveld M, Cutter DJ *et al.* Radiation dose-response relationship for risk of coronary heart disease in survivors of Hodgkin lymphoma. *J Clin Oncol* 2016;34:235–43. https://doi.org/10.1200/JCO.2015.63.4444.
10. Jimenez RB, Wright JL, Bellon JR. Beyond mean heart dose: cardiac metrics for the modern era. *Int J Radiat Oncol Biol Phys* 2022;114:140–2. https://doi.org/10.1016/j.ijrobp.2022.05.011.
11. Poortmans PM, Struikmans H, De Brouwer P *et al.* Side effects 15 years after lymph node irradiation in breast cancer: randomized EORTC trial 22922/10925. *J Natl Cancer Inst* 2021;113:1360–8. https://doi.org/10.1093/jnci/djab113.
12. Niska JR, Thorpe CS, Allen SM *et al.* Radiation and the heart: systematic review of dosimetry and cardiac endpoints. *Expert Rev Cardiovasc Ther* 2018;16:931–50. https://doi.org/10.1080/14779072.2018.1538785.
13. Jaworski C, Mariani JA, Wheeler G *et al.* Cardiac complications of thoracic irradiation. *J Am Coll Cardiol* 2013;61:2319–28. https://doi.org/10.1016/j.jacc.2013.01.090.
14. Saiki H, Petersen IA, Scott CG *et al.* Risk of heart failure with preserved ejection fraction in older women after contemporary radiotherapy for breast cancer. *Circulation* 2017;135:1388–96. https://doi.org/10.1161/CIRCULATIONAHA.116.025434.
15. Saiki H, Moulay G, Guenzel AJ *et al.* Experimental cardiac radiation exposure induces ventricular diastolic dysfunction with preserved ejection fraction. *Am J Physiol Heart Circ Physiol* 2017;313:H392–407. https://doi.org/10.1152/ajpheart.00124.2017.
16. Cuculich PS, Schill MR, Kashani R *et al.* Noninvasive cardiac radiation for ablation of ventricular tachycardia. *N Engl J Med* 2017;377:2325–36. https://doi.org/10.1056/NEJMoa1613773.
17. Robinson CG, Samson PP, Moore KMS *et al.* Phase I/II trial of electrophysiology-guided noninvasive cardiac radioablation for ventricular tachycardia. *Circulation* 2019;139:313–21. https://doi.org/10.1161/CIRCULATIONAHA.118.038261.
18. van der Ree MH, Blanck O, Limpens J *et al.* Cardiac radioablation-a systematic review. *Heart Rhythm* 2020;17:1381–92. https://doi.org/10.1016/j.hrthm.2020.03.013.
19. Pedersen LN, Valenzuela Ripoll C, Ozcan M *et al.* Cardiac radiation improves ventricular function in mice and humans with cardiomyopathy. *Med* 2023;4:928–943.e5. https://doi.org/10.1016/j.medj.2023.10.006.
20. Yan X, Sasi SP, Gee H *et al.* Cardiovascular risks associated with low dose ionizing particle radiation. *PLoS One* 2014;9:e110269. https://doi.org/10.1371/journal.pone.0110269.
21. Sasi SP, Yan X, Zuriaga-Herrero M *et al.* Different sequences of fractionated low-dose proton and single iron-radiation-induced divergent biological responses in the heart. *Radiat Res* 2017;188:191–203. https://doi.org/10.1667/RR14667.1.
22. Abe T, Saitoh J, Kobayashi D *et al.* Dosimetric comparison of carbon ion radiotherapy and stereotactic body radiotherapy with photon beams for the treatment of hepatocellular carcinoma. *Radiat Oncol* 2015;10:187. https://doi.org/10.1186/s13014-015-0491-8 PMID: 26377092.
23. Shiba S, Shibuya K, Kawashima M *et al.* Comparison of dose distributions when using carbon ion radiotherapy versus intensity-modulated radiotherapy for hepatocellular carcinoma with macroscopic vascular invasion: a retrospective analysis. *Anticancer Res* 2020;40:459–64. https://doi.org/10.21873/anticanres.13974.
24. Ohno T. Particle radiotherapy with carbon ion beams. *EPMA J* 2013;4:9. https://doi.org/10.1186/1878-5085-4-9.
25. Anderle K, Stroom J, Pimentel N *et al.* In silico comparison of photons versus carbon ions in single fraction therapy of lung cancer. *Phys Med* 2016;32:1118–23. https://doi.org/10.1016/j.ejmp.2016.08.014.
26. Constantinescu A, Lehmann HI, Packer DL *et al.* Treatment planning studies in patient data with scanned carbon ion beams for catheter-free ablation of atrial fibrillation. *J Cardiovasc Electrophysiol* 2016;27:335–44. https://doi.org/10.1111/jce.12888.
27. Amino M, Yamazaki M, Yoshioka K *et al.* Heavy ion irradiation reduces vulnerability to atrial tachyarrhythmias—gap junction and sympathetic neural remodeling. *Circ J* 2023;87:1016–26. https://doi.org/10.1253/circj.CJ-22-0527.
28. Amino M, Yoshioka K, Tanabe T *et al.* Heavy ion radiation up-regulates Cx43 and ameliorates arrhythmogenic substrates in hearts after myocardial infarction. *Cardiovasc Res* 2006;72:412–21. https://doi.org/10.1016/j.cardiores.2006.09.010.
29. Amino M, Yoshioka K, Fujibayashi D *et al.* Year-long upregulation of connexin43 in rabbit hearts by heavy ion irradiation. *Am J Physiol Heart Circ Physiol* 2010;298:H1014–21. https://doi.org/10.1152/ajpheart.00160.2009.
30. Amino M, Yoshioka K, Furusawa Y *et al.* Inducibility of ventricular arrhythmia 1 year following treatment with heavy ion irradiation in dogs with myocardial infarction. *Pacing Clin Electrophysiol* 2017;40:379–90. https://doi.org/10.1111/pace.13031.
31. Lehmann HI, Richter D, Prokesch H *et al.* Atrioventricular node ablation in Langendorff-perfused porcine hearts using carbon ion particle therapy: methods and an in vivo feasibility investigation for catheter-free ablation of cardiac arrhythmias. *Circ Arrhythm Electrophysiol* 2015;8:429–38. https://doi.org/10.1161/CIRCEP.114.002436.
32. Lehmann HI, Graeff C, Simoniello P *et al.* Feasibility study on cardiac arrhythmia ablation using high-energy heavy ion beams. *Sci Rep* 2016;6:38895. https://doi.org/10.1038/srep38895.
33. Amino M, Yoshioka K, Shima M *et al.* Changes in arrhythmogenic properties and five-year prognosis after carbon-ion radiotherapy in patients with mediastinum cancer. *Ann Noninvas Electrocardiol* 2018;23:e12468. https://doi.org/10.1111/anec.12468.
34. Amino M, Wakatsuki M, Mori S *et al.* Case of successful sympathetic nerve modulation by targeted heavy ion radiotherapy for idiopathic ventricular tachycardia. *Ann Noninvasive Electrocardiol* 2024;29:e70020. https://doi.org/10.1111/anec.70020.
35. Higo T, Naito AT, Sumida T *et al.* DNA single-strand break-induced DNA damage response causes heart failure. *Nat Commun* 2017;8:15104. https://doi.org/10.1038/ncomms15104.

36. Pellegrini L, Foglio E, Pontemezzo E *et al.* HMGB1 and repair: focus on the heart. *Pharmacol Ther* 2019;196:160–82. https://doi.org/10.1016/j.pharmthera.2018.12.005.
37. Lippitz BE, Harris RA. A translational concept of immunoradiobiology. *Radiother Oncol* 2019;140:116–24. https://doi.org/10.1016/j.radonc.2019.06.001.
38. Hu P, Zhang D, Swenson L *et al.* Minimally invasive aortic banding in mice: effects of altered cardiomyocyte insulin signaling during pressure overload. *Am J Physiol Heart Circ Physiol* 2003;285:H1261–9. https://doi.org/10.1152/ajpheart.00108.2003.
39. Nagayama T, Hsu S, Zhang M *et al.* Sildenafil stops progressive chamber, cellular, and molecular remodeling and improves calcium handling and function in hearts with pre-existing advanced hypertrophy caused by pressure overload. *J Am Coll Cardiol* 2009;53:207–15. https://doi.org/10.1016/j.jacc.2008.08.069.
40. Bosch L, de Haan JJ, Bastemeijer M *et al.* The transverse aortic constriction heart failure animal model: a systematic review and meta-analysis. *Heart Fail Rev* 2021;26:1515–24. https://doi.org/10.1007/s10741-020-09960-w.
41. Koitabashi N, Danner T, Zaiman AL *et al.* Pivotal role of cardiomyocyte TGF-beta signaling in the murine pathological response to sustained pressure overload. *J Clin Invest* 2011;121:2301–12. https://doi.org/10.1172/JCI44824.
42. Kanai T, Endo M, Minohara S *et al.* Biophysical characteristics of HIMAC clinical irradiation system for heavy-ion radiation therapy. *Int J Radiat Oncol Biol Phys* 1999;44:201–10. https://doi.org/10.1016/S0360-3016(98)00544-6.
43. Furukawa N, Koitabashi N, Matsui H *et al.* DPP-4 inhibitor induces FGF21 expression via sirtuin 1 signaling and improves myocardial energy metabolism. *Heart Vessel* 2021;36:136–46. https://doi.org/10.1007/s00380-020-01711-z.
44. R Core Team. *R: A Language and Environment for Statistical Computing*. Vienna, Austria: R Foundation for Statistical Computing, 2024. https://www.R-project.org/.
45. Zhang DM, Navara R, Yin T *et al.* Cardiac radiotherapy induces electrical conduction reprogramming in the absence of transmural fibrosis. *Nat Commun* 2021;12:5558. https://doi.org/10.1038/s41467-021-25730-0.